

M. P. Hoerling · J. W. Hurrell · T. Xu · G. T. Bates
A. S. Phillips

Twentieth century North Atlantic climate change. Part II: Understanding the effect of Indian Ocean warming

Received: 8 September 2003 / Accepted: 25 February 2004 / Published online: 22 June 2004
© Springer-Verlag 2004

Abstract Ensembles of atmospheric general circulation model (AGCM) experiments are used in an effort to understand the boreal winter Northern Hemisphere (NH) extratropical climate response to the observed warming of tropical sea surface temperatures (SSTs) over the last half of the twentieth Century. Specifically, we inquire about the origins of unusual, if not unprecedented, changes in the wintertime North Atlantic and European climate that are well described by a linear trend in most indices of the North Atlantic Oscillation (NAO). The simulated NH atmospheric response to the linear trend component of tropic-wide SST change since 1950 projects strongly onto the positive polarity of the NAO and is a hemispheric pattern distinguished by decreased (increased) Arctic (middle latitude) sea level pressure. Progressive warming of the Indian Ocean is the principal contributor to this wintertime extratropical response, as shown through additional AGCM ensembles forced with only the SST trend in that sector. The Indian Ocean influence is further established through the reproducibility of results across three different models forced with identical, idealized patterns of the observed warming. Examination of the transient atmospheric adjustment to a sudden “switch-on” of an Indian Ocean SST anomaly reveals that the North Atlantic response is not consistent with linear theory and most likely involves synoptic eddy feedbacks associated with changes in the North Atlantic storm track. The tropical SST control exerted over twentieth century regional climate underlies the importance of determining the future course of tropical SST for regional climate change and

its uncertainty. Better understanding of the extratropical responses to different, plausible trajectories of the tropical oceans is key to such efforts.

1 Introduction

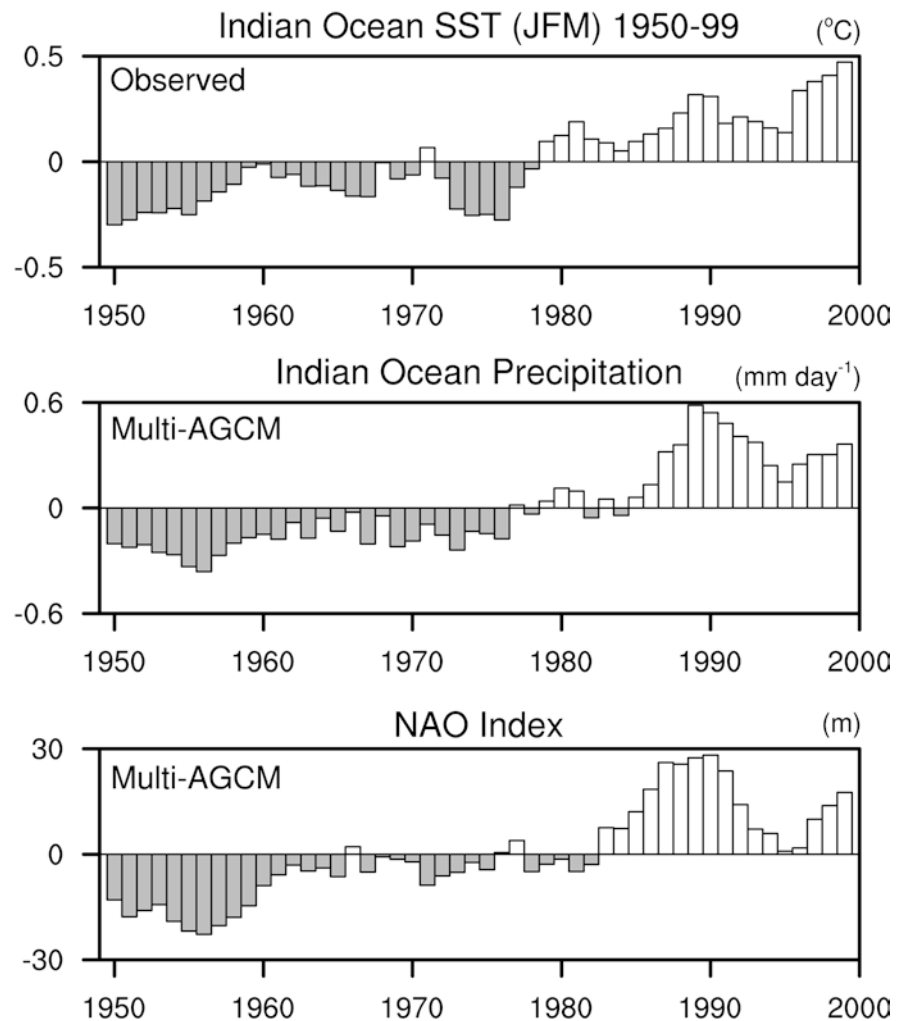
It now appears incontrovertible that the evolution of global sea surface temperatures (SSTs) since 1950 has exerted an important controlling effect on observed North Atlantic climate change. Key evidence is the reproducibility of the observed trend pattern, which resembles the positive index polarity of the North Atlantic Oscillation (NAO), across a range of climate models forced with prescribed, global SSTs (Hurrell et al. 2004; Sutton and Hodson 2003; Mehta et al. 2000; Rodwell et al. 1999). In the first part of this study, Hurrell et al. (2004, hereafter P1) confirm the polarity of this trend pattern to have been a virtually deterministic response to the global ocean in so far as a positive NAO index trend occurs in 58 of 67 individual climate simulations collected from four different atmospheric general circulation models (AGCMs).

A key piece of evidence that changes in tropical SSTs are the principal source for the extratropical trends comes from an ensemble experiment with one of the models forced with observed SSTs within tropical latitudes (30°N–30°S) only. It, too, reproduced the observed atmospheric trend pattern of North Atlantic climate (see also Hoerling et al. 2001). It is thus reasonable to ask whether the atmospheric trends simulated in other models using global SSTs primarily reflect the history of tropical forcing. Lin et al. (2002) and Lu et al. (2004) provide independent, observational support for such an argument. They too used an AGCM, but forced it with the distribution of atmospheric diabatic heating anomalies computed from observed circulation statistics for each of the 51 winters during 1949–1999. The global pattern of this interannually varying diabatic forcing

M. P. Hoerling (✉) · T. Xu · G. T. Bates
Climate Diagnostics Center NOAA,
325 Broadway Boulder, Boulder,
CO 80305-3328, USA
E-mail: martin.hoerling@noaa.gov

J. W. Hurrell · A. S. Phillips
National Center for Atmospheric Research,
Boulder, CO, USA

Fig. 1 Time series (1950–99) of seasonal (January–March) anomalies of observed Indian Ocean (15°S–15°N, 40°E–110°E) SSTs (*top*, °C), multi-AGCM simulated Indian Ocean precipitation (*middle*, mm day⁻¹), and multi-AGCM simulated North Atlantic Oscillation (NAO) index (*bottom*, m). The latter is the difference in 500 hPa heights averaged over a southern (30°N–50°N, 80°W–20°E) minus a northern (60°N–80°N, 80°W–20°W) domain. The model data are the ensemble means of 67 GOGA members across four different AGCMs (see text for details). All anomalies are relative to the respective JFM 1950–99 climatologies



was used in one ensemble of experiments, while only the tropical portion was used in a second ensemble. Both experiments realistically simulate the observed change in North Atlantic climate, a response associated with a pattern of enhanced diabatic heating south of the equator spanning the Indian Ocean to the tropical South Atlantic Ocean, and one resembling the 1950–1999 rainfall trends simulated in the four AGCMs studied in P1.

From these results, the question arises about the cause for the trend in the tropical diabatic forcing. Can it be understood as the response to only the trend component of the tropical SSTs themselves? More importantly, can North Atlantic/European climate change during this period be understood as the remotely

forced atmospheric response to this SST trend component and, if so, which of the tropical SST changes are most relevant?

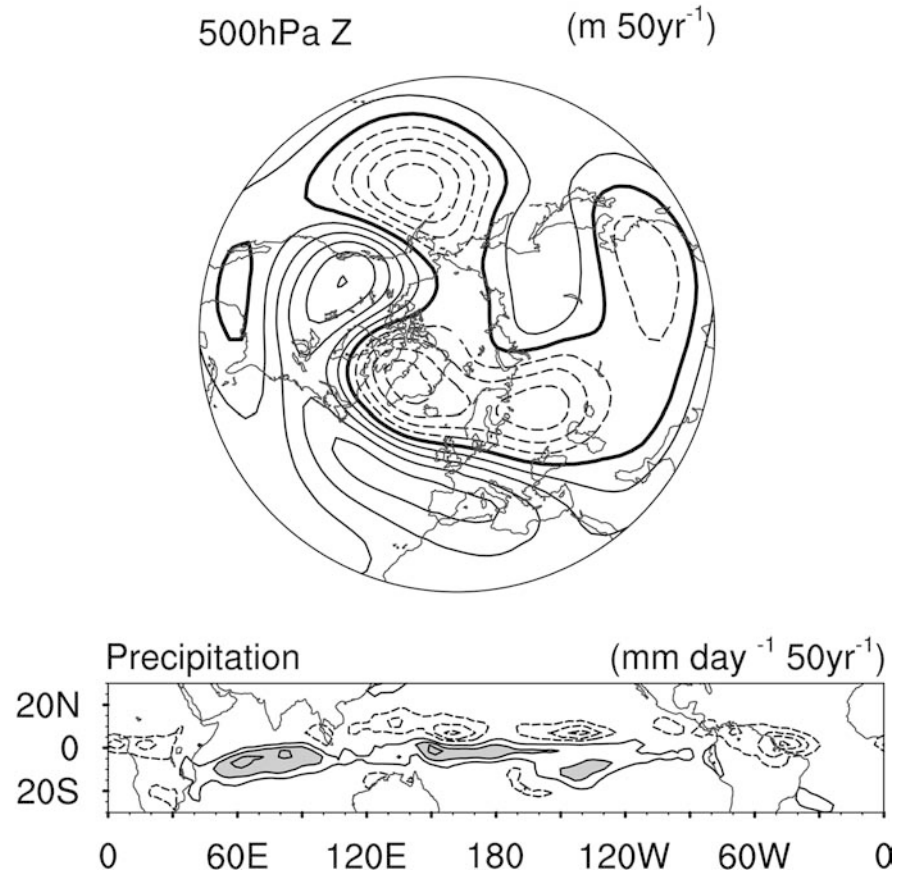
There are some clues from existing AGCM simulation studies. In particular, two different climate models indicate that the history of tropical Atlantic SSTs since 1950 have not contributed to the North Atlantic climate trend (P1; Sutton and Hodson 2003), even though their interannual fluctuations do contribute to North Atlantic seasonal atmospheric variability (Venzke et al. 1999; Sutton et al. 2001). The experiments of Sutton and Hodson (2003) spanned 1871–1999, from which they detected a tropical Indo-Pacific SST contribution to the upward NAO index trend of recent decades. Similarly, Bader and Latif (2003) forced their AGCM with an

Table 1 Idealized SST forcing and AGCM ensemble sizes

	Tropic-Wide Trend	Tropical E. Hemisphere Trend	Tropical Indian Ocean Trend	Equilibrium +1 °C Indian Ocean	Transient +1 °C Indian Ocean
CCM3	20	20	20	20	100
NSIPP-1				40	
GFS				40	

Fig. 2 The linear trend (1950–99) of the January–March multi-AGCM ensemble mean (*top*) 500 hPa heights and (*bottom*) total tropical precipitation. The ensemble means were computed from 67 individual GOGA simulations across four different AGCMs (see text for details). The contour increment for the height trend is 6 m per 50 years, the zero contour is given by the *thick dark line*, and negative trends are *dashed*. The contour increment is $1.0 \text{ mday}^{-1} 50 \text{ year}^{-1}$ for the precipitation trend, the zero contour is omitted, negative trends are *dashed*, and trends exceeding $+2.0 \text{ mday}^{-1} 50 \text{ year}^{-1}$ are *shaded*

Linear Trend (JFM) Multi-AGCM 1950-99



observed decadal change pattern of Indian Ocean SSTs only and found a strong NAO response of the same sign as that observed, and Lu et al. (2004) concluded the trend in the NAO has been driven by forcing in the Indo-Pacific region. These studies thus appear to support the hypothesis of Indian Ocean forcing of recent North Atlantic climate change originally proposed in Hoerling et al. (2001). The possible importance of forcing from that sector is further quantified in the first part of this study (P1), where we found that monthly rainfall variations over the Indian Ocean coincide with occurrences of the positive polarity of the NAO in four different AGCMs. Likewise, recent AGCM studies examining the extratropical impacts of the unusually warm Indian Ocean state observed during boreal winter 1997–1998 have also documented a response projecting onto the positive polarity of the NAO (Ferrara et al. 2000; Pegion et al. 2001), as have Hoerling and Kumar (2003) in their study of the origins of the Mediterranean drought that has persisted since 1998.

We thus specifically and methodically explore in this paper whether the Indian Ocean has been the principal tropical contributor to the North Atlantic climate change of the last half-century. A further motivation for

such a pursuit is the striking similarity among time series of Indian Ocean and North Atlantic climate variations since 1950 (Fig. 1). The January–March (JFM) seasonal SSTs averaged over the tropical Indian Ocean (15°S – 15°N , 40°E – 110°E) have increased $0.60 \pm 0.10^{\circ}\text{C}$ since 1950, with most of the warming occurring in the last 30 years (top panel). This has likely caused rainfall to increase over the same domain (Fig. 12 of P1), as estimated from the aforementioned 67-member multi-AGCM ensemble (middle panel). The temporal behavior of the multi-AGCM JFM NAO index is also very similar (bottom panel), suggesting that the Indian Ocean warming trend may be a crucial forcing. These relationships are only anecdotal evidence for a causal link, however, as they have been derived from AGCM simulations using global SST forcing (Global Ocean Global Atmosphere, or GOGA, simulations). The apparent binding of trends over the Indian Ocean and North Atlantic sectors may be entirely coincidental, as suggested for instance by Schneider et al. (2003).

In the next section we describe a new suite of AGCM experiments that employ idealizations of the temporal changes in tropical SST forcing over the last half of the twentieth Century. In particular, we seek to understand

Responses (JFM) to Tropical SST Trends 1950-99

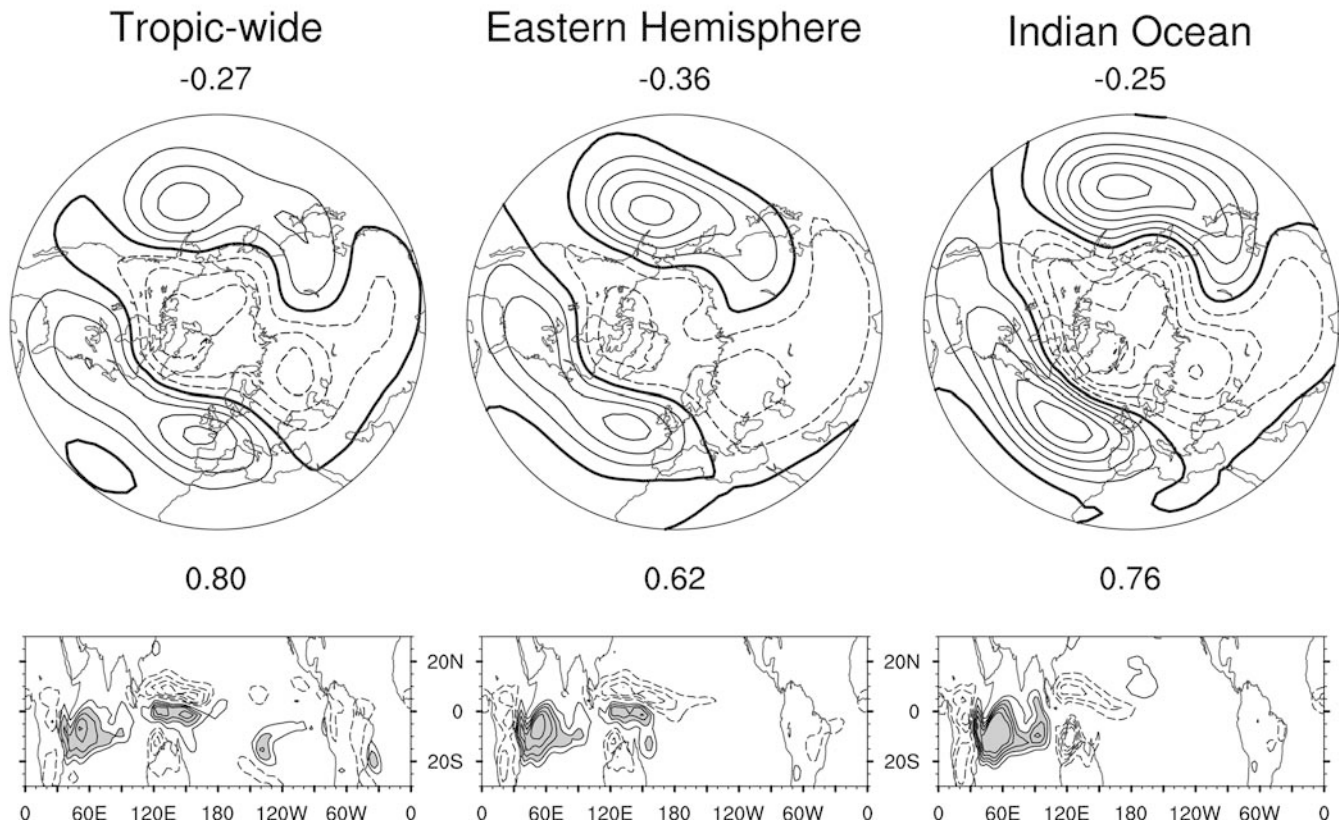


Fig. 3 Ensemble mean atmospheric responses (January–March) of 500 hPa heights (*top*, m) and tropical precipitation (*bottom*, mm day^{-1}) to trend components (1950–99) of observed tropic-wide SSTs (*left*), tropical Eastern Hemisphere SSTs (*middle*), and tropical Indian Ocean SSTs (*right*, see text for details). Anomalies are relative to the NCAR CCM3 climatology from a control simulation with a repeating seasonal cycle of mean (1971–2000) SSTs. Numbers plotted above (*below*) the 500 hPa height responses

are the spatial correlations with the multi-AGCM GOGA trends (*top*, Fig. 2) for the North Pacific (North Atlantic) half of the Northern Hemisphere (see text for further details). The contour increment for the height responses is 15 m, the zero contour is indicated by the *thick black line*, and negative responses are *dashed*. For precipitation, the contour increment is 1.0 mm day^{-1} , the zero contour is omitted, negative responses are *dashed*, and responses exceeding $+2.0 \text{ mm day}^{-1}$ are *shaded*.

whether the grossest aspect of that change, namely the linear trend, can alone account for the North Atlantic atmospheric changes derived from GOGA experiments (e.g., Fig. 1). The results from a trilogy of such ensemble simulations are presented in Sect. 3. These experiments establish that the observed trends in various indices of North Atlantic climate since 1950 can indeed be viewed as the response to the linear warming trend of the tropical oceans, with SST warming over the Indian Ocean sector as the key forcing. Explored in Sect. 4 is the robustness of these results, in terms of the atmospheric sensitivity to an idealized $+1 \text{ }^\circ\text{C}$ Indian Ocean SST anomaly across three different AGCMs. The atmospheric responses are shown to be in close agreement, not only between models but also with the SST trend runs of Sect. 3, thus supporting the interpretation of Fig. 1 as the atmospheric response to Indian Ocean warming. To understand the mechanistic aspects of this remote influence, we also study the transient atmospheric adjustment to the idealized Indian Ocean

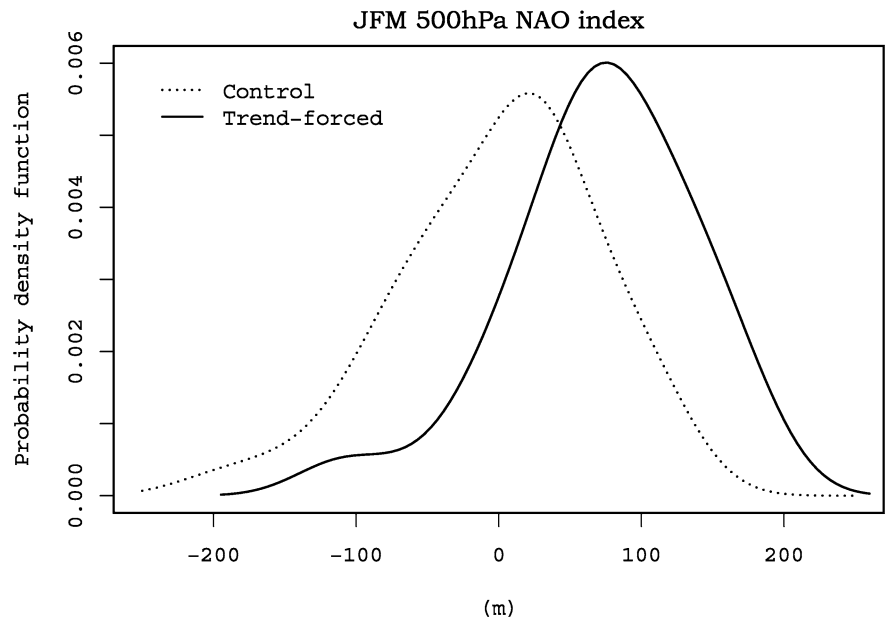
warming. We summarize the principal findings in Sect. 5, which concludes with a discussion of the relevance of our findings to improved understanding of sources of uncertainty in projections of future regional climate change.

2 Data and methodology

2.1 Sea surface temperature

There are several sources of the monthly SST analyses used to force the different AGCMs examined in P1, and differences among them reflect uncertainties in the knowledge of this important climate parameter. Over the tropics, however, it is notable that the agreement is best, as all products capture the large interannual climate swings associated with the ElNiño/Southern Oscillation (ENSO) phenomenon, and most exhibit similar warming trends since 1950 (e.g., Hurrell and

Fig. 4 Empirical probability distribution function (PDF) of January–March (JFM) North Atlantic Oscillation (NAO) index values. The data given by the *solid line* are from 60 individual NCAR CCM3 responses, projected onto the NAO pattern, to three tropical SST trend experiments (see text and Fig. 3). The *dotted curve* is the PDF from a 120-year control simulation with a repeating seasonal cycle of mean (1971–2000) SSTs. The NAO index is defined as in Fig. 1



Trenberth 1999). In this part of the study, observed monthly SSTs are analyzed at two-degree resolution over 1950–1999, obtained by merging the empirical orthogonal function reconstructed analyses of Smith et al. (1996) with the optimal interpolation (OI) SST analyses of Reynolds and Smith (1994). The latter are available since late 1981 and consist of both *insitu* and bias-corrected satellite-derived SSTs.

2.2 AGCM experiments

Table 1 summarizes the suite of new ensemble experiments we study, in terms of their ensemble size and the various idealizations of the SST used to force the models. Three different AGCMs were forced with the identical SST anomaly pattern in one experiment, in order to evaluate the model dependency of the atmospheric response. Further details on the models themselves are provided in Table 1 of P1.

The intent of the first set of experiments was to determine the atmospheric response during boreal winter to the linear trend component of tropical SST forcing, and in particular to the warming trend of the Indian Ocean surface temperatures in recent decades (Fig. 1). The amplitude of the specified SST anomalies in these simulations was given by the 1950–1999 linear trend, scaled to °C change over 50 years. The calculation, performed within 25°S–25°N, was done for three-month running seasons and added to the seasonally varying climatology, thereby yielding an estimate of the incremental change in tropical SSTs throughout the annual cycle during the last half of the twentieth Century. This calculation for the JFM season (see Fig. 6 of P1), plus the SST anomaly patterns for the other 11 overlapping three-month seasons were used in the first AGCM ensemble set of a trilogy. The second ensemble set

employed the SST trend patterns between 30°E–160°E only, while the third used just the Indian Ocean (40°E–110°E) anomaly components. A total of 20 14-month simulations, beginning from randomly selected 1 November atmospheric initial conditions, were performed for each scenario. The model used was version three of the NCAR Community Climate Model (CCM3; Kiehl et al. 1998).

Additional ensembles of experiments were conducted using an Indian Ocean only SST forcing having a maximum amplitude of +1 °C between 5°S–5°N, reduced to zero amplitude at 25° latitude. This anomaly pattern, fixed throughout the seasonal cycle and added to the seasonal climatological SST field, was prescribed to cover the entire zonal width of the tropical Indian Ocean as an idealization of the 1950–1999 observed change in that sector. A total of 20 14-month simulations, beginning from randomly selected 1 November atmospheric initial conditions, were performed with CCM3. To assess the robustness of results across models, a second ensemble set of 20 18-month simulations (yielding 40 winter samples) was performed using the identical anomalous SST forcing, but with the model of the NASA Seasonal-to-Interannual Prediction Project (NSIPP-1; Schubert et al. 2003). Also, a third 40-member ensemble of experiments with the same forcing was performed using the National Centers for Environmental Predictions (NCEP) climate model (GFS). (The NSIPP-1 experiments and data were kindly provided by Drs. P. Pegion, M. Suarez, and S. Schubert, while Drs. B. Bhaskar and A. Kumar provided the GFS data). All anomalies were calculated relative to long control integrations of the respective models that used only the repeating seasonal cycle of climatological SSTs.

Finally, another set of experiments was performed with the NCAR CCM3, and these were constructed to illustrate the transient atmospheric adjustment to a

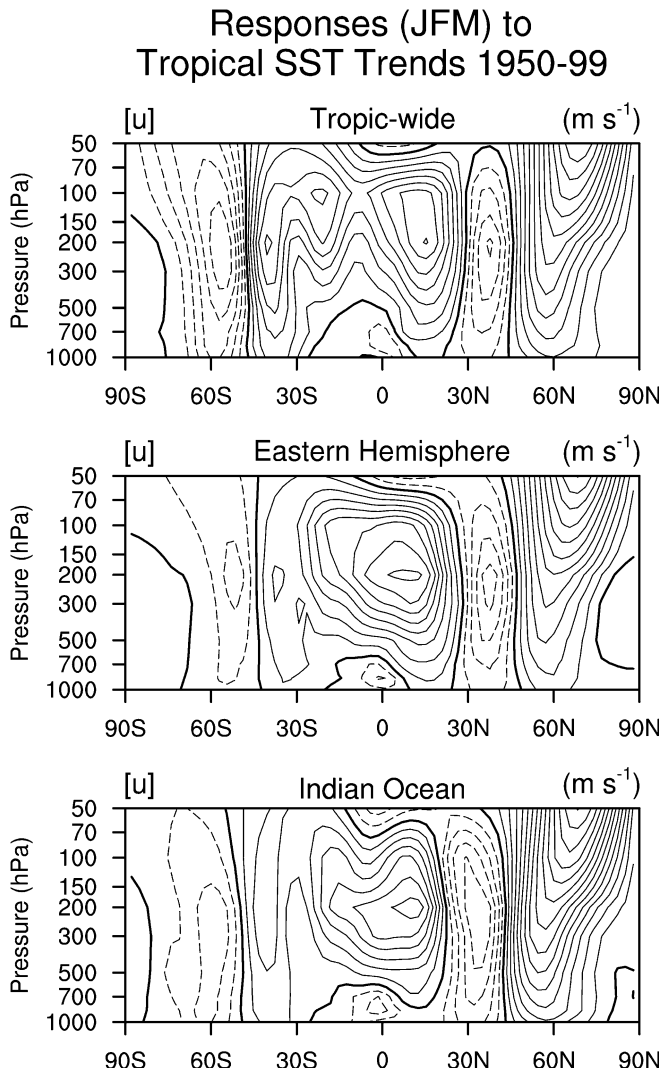


Fig. 5 Vertical cross sections of the January–March response of the zonal mean zonal wind to the three tropical SST trend experiments (see text and Fig. 3). Contours, every 0.5 m s^{-1} , are *solid* (*dashed*) for positive (negative) values. Anomalies are with respect to the control climatology of the NCAR CCM3 using a repeating seasonal cycle of mean (1971–2000) SSTs

sudden “switch-on” of the idealized $+1 \text{ }^\circ\text{C}$ Indian Ocean SST anomaly pattern. In particular, an ensemble of 100 runs with the anomalous forcing, each begun from randomly selected 1 January atmospheric initial conditions, was compared to an ensemble of the same size created from only climatological SST forcing. The simulations were of 45-day duration, by which time the atmospheric anomalies were equilibrated. The daily evolving differences in atmospheric states between these parallel ensemble averages are analyzed in Sect. 4.

3 Atmospheric response to trends in tropical SST

Our purpose is to interpret the simulated 1950–1999 trends of 500 hPa heights and precipitation occurring in AGCMs forced by the complete monthly history of

global SSTs. The Northern Hemisphere (NH) JFM seasonal trends based on the 67-member multi-model GOGA ensemble mean of P1 (Fig. 2) are compared subsequently to AGCM experiments using various idealizations of the observed tropical SST variability.

The ensemble averaged 500 hPa height and tropical rainfall responses to the 1950–1999 SST trend component forcings, specified over the entire tropics (left panels), the tropical eastern Hemisphere (middle panels), and the tropical Indian Ocean (right panels), are shown in Fig. 3. The outstanding characteristic of the boreal winter North Atlantic height response in all three forcing experiments is the strong and robust projection onto the positive polarity of the NAO pattern. The similarity between these trend-forced patterns and that driven by the full time history of global SSTs (Fig. 2) is quantified through spatial correlations, as listed in Fig. 3 beneath the 500 hPa responses. Over the North Atlantic half of the NH (90°W – 90°E , 20°N – 90°N), these range from 0.62 to 0.80.

As a measure of the statistical robustness of this circulation response, the projection of 500 hPa height anomalies onto an NAO index has been computed for each of the 60 realizations comprising the three experiments¹. The estimated probability density function (PDF) of the NAO index (Fig. 4) reveals that more than 80 percent of the trend realizations generate a positive projection onto the NAO pattern, with a mean response of 72 m that is significantly different from zero at the 99% level. This mean response is comparable to the ensemble mean value of the 1950–1999 NAO index trend of 44 m simulated in the multi-AGCM GOGA ensembles of P1 (see their Fig. 4).

These results indicate that the spatial pattern of North Atlantic climate change since 1950 is consistent with the dynamical response of the atmosphere to the trend component of tropical SST change, and that the statistics of the higher frequency interannual SST variability are not of primary importance. It is further revealed that the trend component of tropical Indian Ocean surface temperature is most relevant, alone being sufficient to explain the response pattern over the North Atlantic and European region. The simulated 500 hPa responses to the tropical-wide and the Indian Ocean only SST trends correlate at 0.9 over the NH poleward of 20°N .

The similarity among the winter ensemble mean NH extratropical circulation responses of the three trend experiments is consistent with the fact that their ensemble mean tropical rainfall anomalies are also very similar, suggesting that the effective forcing from the tropics is analogous (Fig. 3, bottom panels). These are distinguished by increased equatorial rainfall over the eastern Hemisphere, flanked by drying over the tropical western Pacific and over Africa. This pattern, moreover, reproduces the regional rainfall trends captured in the

¹The index for the North Atlantic Oscillation is defined as in P1. It is the difference between 500 hPa heights averaged over a southern (30°N – 50°N , 80°W – 20°E) and a northern (60°N – 80°N , 80°W – 20°W) domain.

Responses (JFM) to Tropical SST Trends 1950-99

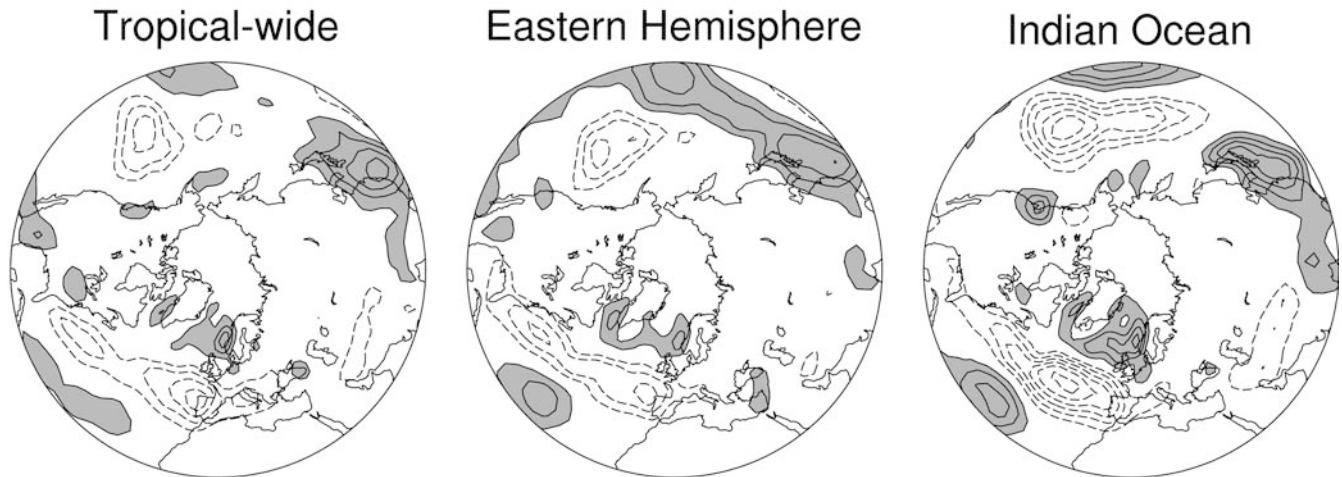


Fig. 6 Ensemble mean precipitation responses (January–March) over the Northern Hemisphere extratropics to the three tropical SST trend experiments (see text and Fig. 3). Contours are every 0.25 mm day^{-1} , the zero contour is omitted, and positive (negative)

responses are shaded (dashed). Anomalies are with respect to the control climatology of the NCAR CCM3 using a repeating seasonal cycle of mean (1971–2000) SSTs

AGCM experiments of P1 (Fig. 2). We thus interpret their origin to be the linear component of the progressive warming of ocean surface temperatures over the “warm pool” of the Indian and western Pacific Oceans.

In contrast, the idealized SST experiments fail to reproduce the substantial increase in rainfall over the tropical central and eastern Pacific Ocean evident in the simulations of P1. The statistics of interannual SST variations over this region, especially those related to ENSO, are evidently more important. Furthermore, it is reasonable to presume that the failure to reproduce this regional rainfall increase explains the disagreement in the Pacific–North American (PNA) 500 hPa circulation responses (compare Figs. 2 and 3). Whereas the regional NAO trend pattern evident in the GOGA experiments is seen in the response to the tropical SST trend forcing alone, only the former exhibits a discernable positive PNA-component. This disagreement is quantified through the spatial correlations of the responses, computed over $90^{\circ}\text{E}–90^{\circ}\text{W}$, $20^{\circ}\text{N}–90^{\circ}\text{N}$ and listed above the 500 hPa responses of Fig. 3. In striking contrast to those over the North Atlantic sector, these correlations range from -0.25 to -0.36 . The trend in North Pacific and North American climate since 1950 cannot therefore be reconciled with the extratropical response to only the trend component of tropical SSTs, and it is plausible that it reflects the important influence of temporal fluctuations of ENSO since 1950. A more detailed analysis of this problem will appear in a separate paper.

For the NH extratropics as a whole, the wintertime circulation response to the trend component of tropical SST change has a notable zonally symmetric component. The zonally averaged zonal wind response in the three trend experiments (Fig. 5) reflects a poleward shift of the NH middle latitude westerlies throughout the

depth of the troposphere and lower stratosphere. This response is very similar to the zonal wind structure that characterizes the positive polarity of the Northern Annular Mode (NAM), as shown by the composites of Thompson et al. (2003), although the simulated tropical westerly wind response is of larger amplitude. These results indicate that a NAM-like structure can be efficiently forced from the tropics, raising the possibility that recent observed trends in the NAM (Thompson et al. 2000) are not only consistent with, but are perhaps driven by, the warming trend of tropical waters.

Accompanying the simulated poleward shift in the NH boreal winter westerlies is an increase in precipitation within the zonal band $50^{\circ}\text{N}–70^{\circ}\text{N}$ and a decrease within $40^{\circ}\text{N}–50^{\circ}\text{N}$ (Fig. 6). The responses are strongest along and downstream of the wintertime westerly maxima, and thus likely are associated with poleward shifts in storm track activity. As a signature of a poleward displacement of moisture bearing storms, a dipole precipitation pattern is particularly evident over the North Atlantic and European region in the three trend experiments. Drying over the Mediterranean and southern Europe together with increased precipitation over Scandinavia and northern Europe realistically captures both the observed regional trend pattern since 1950 and the simulated rainfall trends in the global SST forcing experiments of P1 (see their Fig. 5).

4 Atmospheric response to Indian Ocean warming

4.1 Equilibrium response

These results from the SST trend experiments advance the argument for a link between forcing over the Indian

Responses (JFM) to +1°C Indian Ocean SST Anomaly

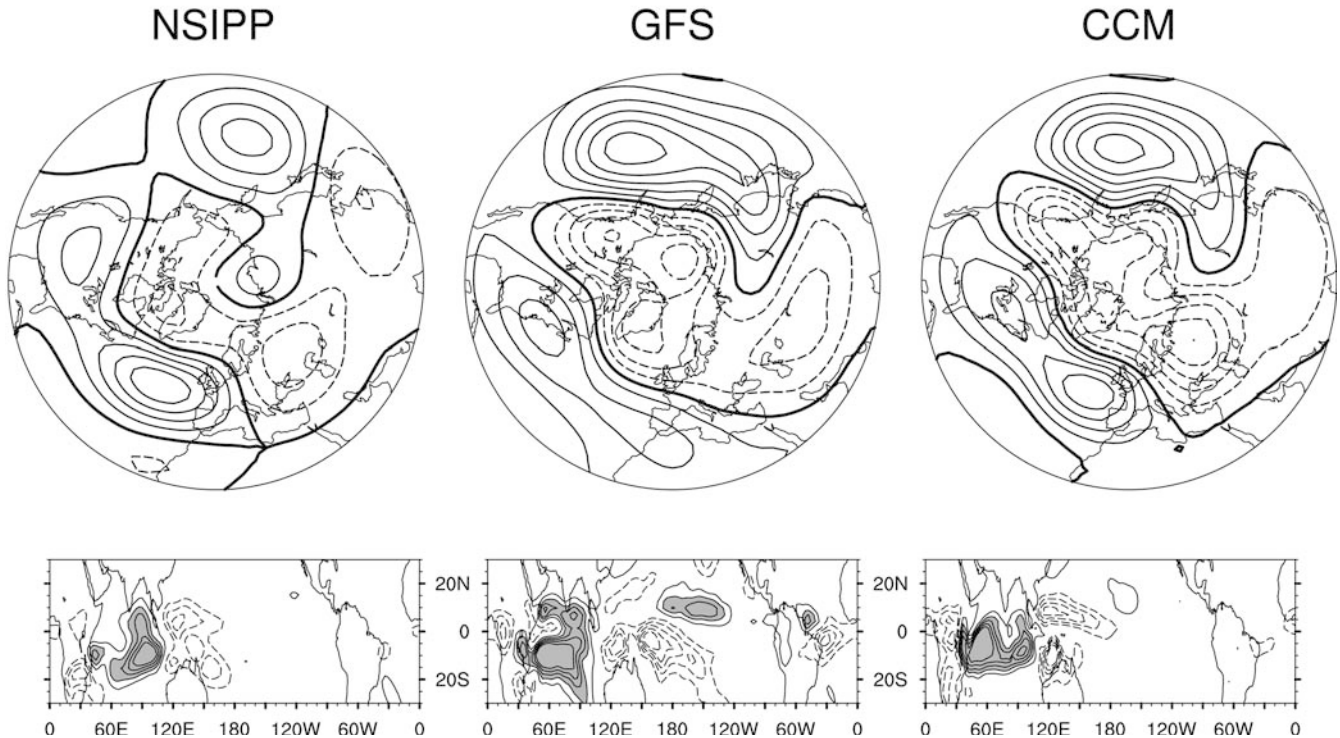


Fig. 7 Ensemble mean atmospheric responses (January–March) of 500 hPa heights (*top*, m) and tropical precipitation (*bottom*, mm day⁻¹) to a +1°C warming of the tropical Indian Ocean (see text for details). The responses of the NASA NSIPP-1 (*left*), NCEP GFS (*middle*) and NCAR CCM3 (*right*) AGCMs are all relative to their respective climatologies from control simulations

with repeating seasonal cycles of mean (1971–2000) SSTs. The contour increment for the height responses is 15 m, the zero contour is indicated by the *thick black line*, and negative responses are *dashed*. For precipitation, the contour increment is 1.0 mm day⁻¹, the zero contour is omitted, negative responses are *dashed*, and responses exceeding +2.0 mm day⁻¹ are *shaded*

Ocean and an extratropical response over the North Atlantic region. We further diagnose the realism and robustness of such a relationship by performing suites of idealized +1°C Indian Ocean warming experiments with three different AGCMs. Figure 7 displays each model's JFM ensemble mean 500 hPa height and tropical rainfall responses, with the NCAR CCM3 displayed on the right side. Note that its response virtually replicates that of Fig. 3, further establishing its statistical robustness and confirming that the idealized +1°C forcing is a useful approximation to the actual 1950–1999 Indian Ocean SST trend.

Importantly, the ensemble anomalies of the other two atmospheric models bear considerable resemblance to those of CCM3. The spatial correlation of the NSIPP-1 and GFS responses with that of CCM3 (averaged poleward of 20°N) is 0.78 and 0.79, respectively. Indicated hereby is that the influence of the Indian Ocean on the NH extratropical circulation is not unduly dependent upon arbitrary choices among these particular models, and that the teleconnection is very likely a fundamental property of true atmospheric sensitivity. Regional differences among the three response patterns are akin to the inter-model differences in 1950–1999 500 hPa height trends with global SST forcing noted in

P1. Yet, each yields a response pattern which projects strongly on the positive polarities of the NAO/ NAM patterns.

The three NH precipitation responses are a further assessment of model sensitivities (Fig. 8). The most prominent and reproducible features are the zonally elongated bands of drying over the middle latitude oceans that appear to be signatures of poleward displaced storm track activity along and downstream of the Pacific and Atlantic westerly maxima. This is accompanied by drying of the southern European and Mediterranean region and increased precipitation over northern Europe and Scandinavia in all three AGCMs, a behavior consistent with the NAO-like regional circulation responses, and a sensitivity that is remarkably similar to observed trends in North Atlantic boreal winter precipitation since the middle of the twentieth Century.

4.2 Transient response

The equilibrium experiments establish a characteristic structure of the NH extratropical response to Indian Ocean warming that consists during winter months of

Responses (JFM) to +1°C Indian Ocean SST Anomaly

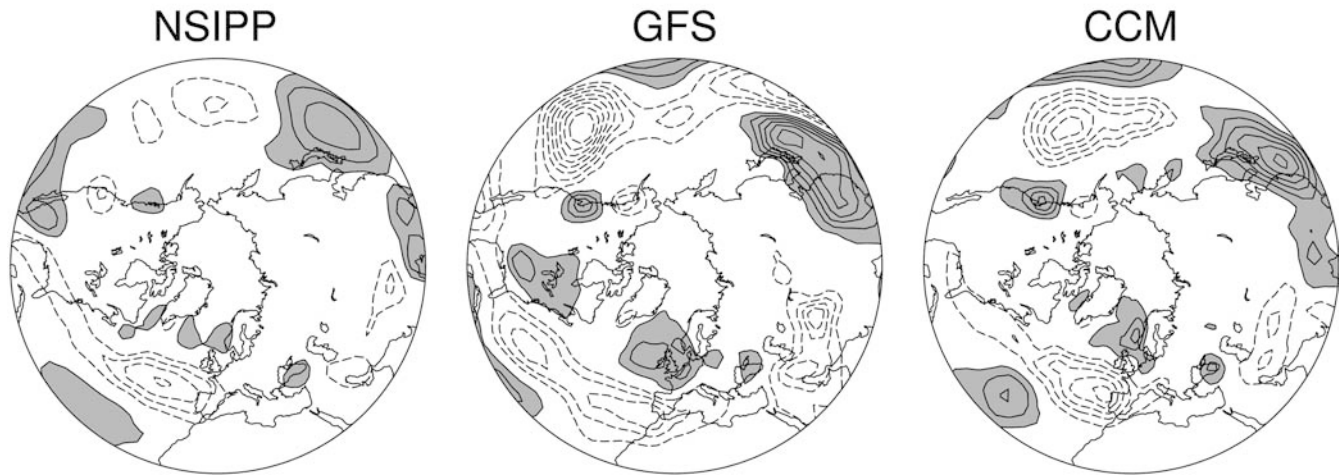


Fig. 8 Northern Hemisphere extratropical ensemble mean precipitation (mm day^{-1}) responses (January–March) to a +1°C warming of the tropical Indian Ocean (see text for details). The responses of the NASA NSIPP-1 (*left*), NCEP GFS (*middle*) and NCAR CCM3 (*right*) AGCMs are all relative to their respective

climatologies from control simulations with repeating seasonal cycles of mean (1971–2000) SSTs. The contour increment is 0.25 mm day^{-1} , the zero contour is omitted, and positive (negative) responses are shaded (dashed)

the positive NAO/NAM index phase. For a forcing strength equal to the observed 50-year change in Indian Ocean SSTs, the amplitude of the response’s projection onto the NAO was found to be comparable to the interannual variations of the NAO index itself. However, while recognizing the robustness and strength of the signal, little more is learned regarding the nature of the teleconnection.

We thus examine the time-dependent response over 45 days, relative to a 1 January start, to a “switch-on” of +1°C Indian Ocean warming in order to elucidate the teleconnection process to which North Atlantic climate is sensitive. Based on the NCAR CCM3 experiments,

the similarity between the days 41–45 anomalies and the January–February (JF) equilibrium response (Fig. 9) confirm that approximate equilibration is achieved by the end of the transient runs. Snapshots of the time evolving 200 hPa height anomalies for consecutive five-day averages during the first 30 days of atmospheric adjustment (Fig. 10) reveal that the incipient response is confined to the Asian sector and, at this upper tropospheric level, consists of a zonally extensive anticyclone positioned poleward of the developing equatorial Indian Ocean heat source. Downstream energy dispersion is implied by the development of a wave train after day 10, the spatial structure of which resembles the negative

Fig. 9 Transient (*left*) and equilibrium (*right*) NCAR CCM3 responses of 200 hPa height (m) to a +1°C warming of the tropical Indian Ocean (see text for details). The transient (days 41–45) response is from a 100-member ensemble, relative to a 1 January start, computed as the difference from a control (climatological SST) ensemble of the same size. The equilibrium response consists of the averaged January–February anomalies occurring in a 20-member ensemble whose January–March response is shown in Fig. 7. The contour increment is 30 m, negative values are dashed and the zero contour is indicated by the *thick black line*

Responses to +1°C Indian Ocean SST Anomaly

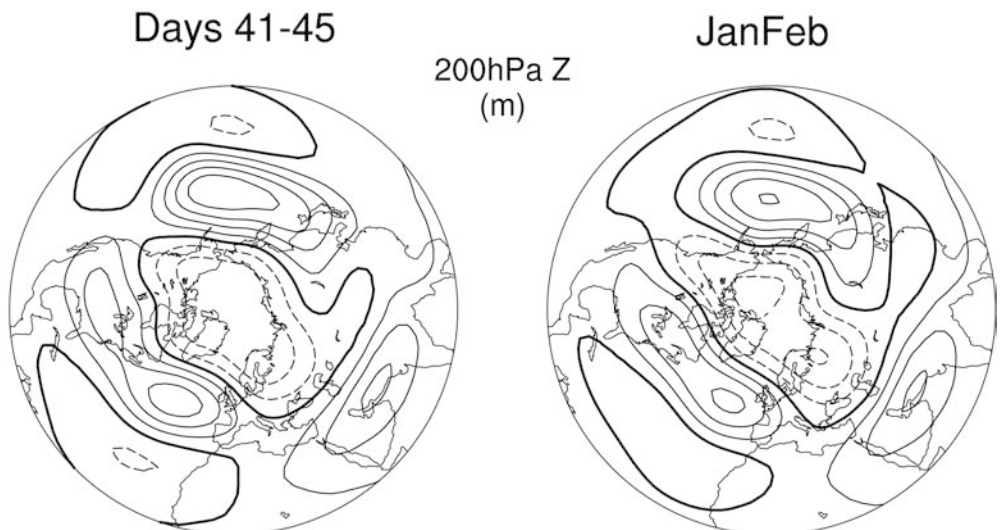
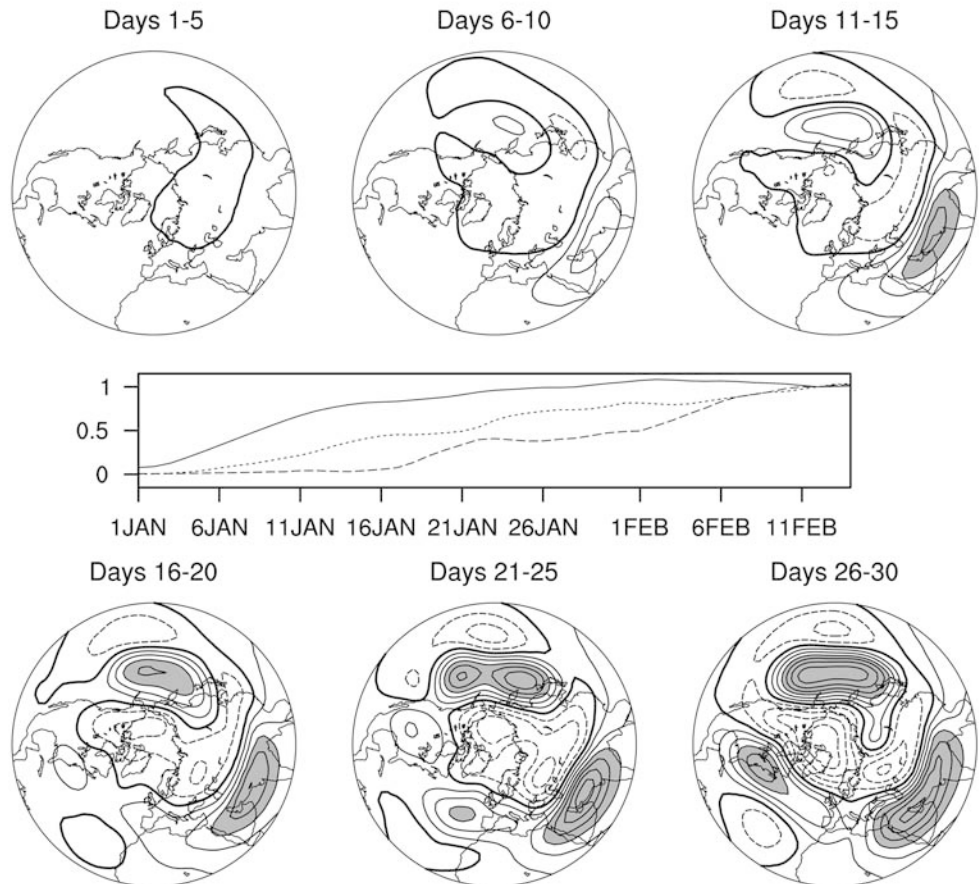


Fig. 10 Transient response of NCAR CCM3 200 hPa height (m) to a +1 °C warming of the tropical Indian Ocean (see text for details). Shown are consecutive 5-averaged anomalies through days 26–30 (*bottom, right*). The insert shows time series (days 1–45) of 200 hPa heights averaged over areas of developing anticyclones: South Asia (10°N–30°N, 40°E–90°E; *solid*), North Pacific (40°N–50°N, 150°E–180°; *dotted*), and North Atlantic (40°N–50°N, 45°W–15°W; *dashed*). The time series anomalies are standardized by their equilibrated values for days 41–45. The contour increment is 15 m, negative values are *dashed*, and responses exceeding +45 m are *shaded*

200hPa Z Response to +1°C Indian Ocean SST Anomaly



polarity of the PNA teleconnection pattern, and its four centers-of-action are clearly visible by the third pentad and beyond.

By contrast, development of the North Atlantic response is deferred until after days 16–20. The time series shown in the insert of Fig. 10 monitor daily 200 hPa height anomalies within the three prominent extratropical anticyclones: over southern Asia, the North Pacific, and the North Atlantic. The amplitude of these time evolving positive height anomalies is standardized by their near-equilibrated values for days 41–45 of the transient integrations. Not surprisingly, the anomalous Asian high (solid line) develops first and rapidly, acquiring 75% of its saturated amplitude by day 16. A more gradual growth occurs for the North Pacific high (dotted line), as it reaches 40% of its peak amplitude by day 16, whereas no discernible North Atlantic response occurs until after day 16.

The circulation anomalies that develop during the first two weeks over Asia and the PNA region appear to be consistent with existing linear theory and the known atmospheric wave dynamics associated with tropical forcing (e.g., Trenberth et al. 1998). The occurrence of the PNA wave pattern emerges, for example, as the preferred linear response of a barotropic model to tropical forcing, one that Simmons et al. (1983) find to be optimally excited

by forcing over Southeast Asia such as occurs in our experiment using an Indian Ocean SST perturbation.

On the other hand, it is unlikely that simple downstream energy dispersion and linear wave theory can explain the subsequent North Atlantic NAO-like response. For example, Simmons et al. (1983) do not find a relation between the response of their barotropic model over the North Atlantic and forcings over Asia. Nor do North Atlantic responses to a specified Indian Ocean heat source occur in the linear and nonlinear baroclinic model experiments of Ting and Yu (1998). It is reasonable to suppose that nonlinear transient eddy feedbacks are important in the adjustment process, in particular over the North Atlantic whose mean jet, and its fluctuations, are believed to be strongly eddy driven (e.g., Thompson et al. 2003; Lee and Kim 2003).

Evidence for the importance of eddy feedbacks is suggested by the time-evolving adjustment of the zonal-mean zonal wind in the transient runs (Fig. 11). Initially, the zonal mean zonal winds accelerate in the subtropics of both hemispheres, signifying a thermally driven response of the subtropical westerlies that occurs immediately poleward of the Indian Ocean heat source. This tendency is subsequently reversed, and by days 21–30, subtropical easterlies have replaced the initial westerlies in the NH. This pattern amplifies further, and the equilibrated state

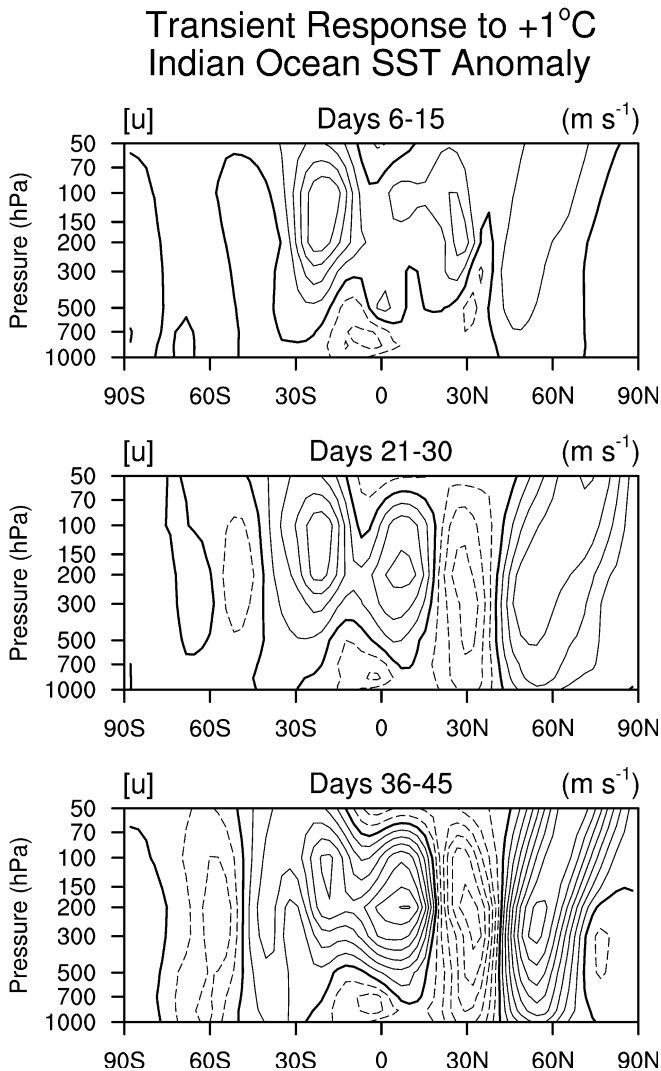


Fig. 11 Vertical cross sections of the NCAR CCM3 transient responses of the zonal mean zonal wind to a +1 °C warming of the tropical Indian Ocean (see text for details). Displayed are 10-day averaged anomalies for days 6–15 (*top*), 21–30 (*middle*), and 36–45 (*bottom*). Contours are 0.25 m s⁻¹ (0.50 m s⁻¹) in the top (*middle* and *lower*) panel, and positive (negative) anomalies are *solid* (*dashed*)

consists of a dipole characterized by subtropical easterly anomalies and subpolar westerly anomalies. Poleward of 20°N, these anomalies have a deep vertical structure, and the vertically integrated zonal momentum balance requires that the tendency at these latitudes be driven by the meridional convergence of zonal momentum by eddies (e.g., Robinson 1992, 1996).

5 Conclusions

5.1 Summary

Given the evidence presented in P1 and elsewhere that North Atlantic climate change during 1950–1999 has been strongly determined by the history of global SSTs,

we have sought to understand what SST behavior was most relevant. New AGCM experiments were analyzed in which the atmosphere was subjected to various idealizations of the observed wintertime tropical SST changes since 1950. Large ensemble experiments were performed and several different atmospheric models were utilized to ensure statistical and physical robustness of results.

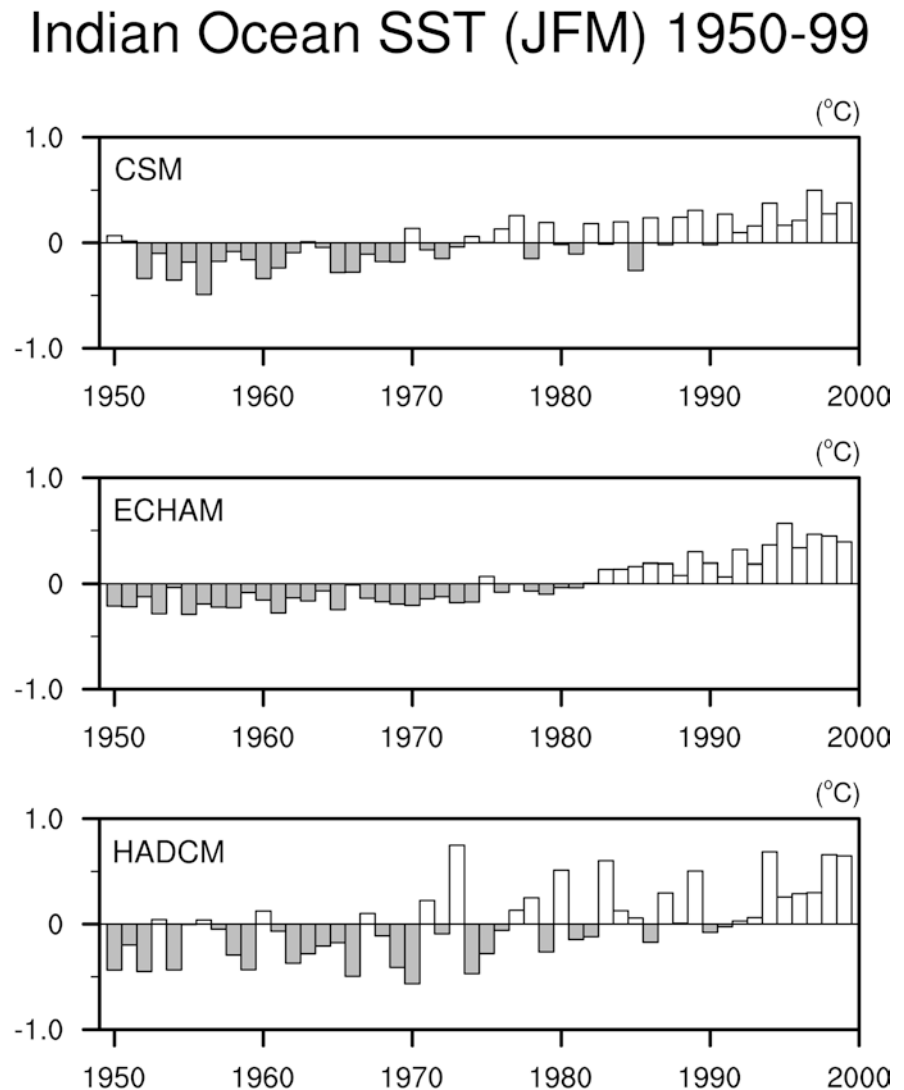
The wintertime North Atlantic sector climate change, well described by a simple linear trend toward the positive index phase of the NAO (P1), was found to correspond with the atmospheric response pattern to the 1950–1999 trend components of tropical SSTs alone. These idealized SST anomaly experiments were shown to reproduce the patterns of North Atlantic climate change occurring in the GOGA simulations of P1, indicating that the detailed history of monthly and interannual SST variations have been of secondary importance.

The warming trend of the Indian Ocean was found to be the most salient of the changes in tropical SSTs. A further suite of experiments using a simple +1 °C Indian Ocean SST anomaly, which is close to the amplitude of the observed 50-year warming trend, was performed using the AGCMs of three different institutions. Each model generated a regional extratropical response that again projected onto the positive polarities of the NAO/NAM pattern. While this indicates a strong degree of robustness across the models, we do note it is in contrast to the recent results of Schneider et al. (2003). They used another AGCM and also examined the extratropical NH response during boreal winter to the recent warming of the tropical oceans. They did not find a link, leading them to conclude that the observed trend in the NAO index likely has been the residual of “interdecadal time scale internal atmospheric noise”. However, it should also be noted that their experiments with the full history of global SST forcing failed to reproduce the observed North Atlantic climate change to the extent captured in the experiments with the four AGCMs examined in P1, as well as with the model of Rodwell et al. (1999). The Schneider et al. (2003) conclusions are also at odds with the AGCM studies of Lin et al. (2002) and Lu et al. (2004).

We thus conclude that the tantalizing similarity of trend components in the NAO and Indian Ocean SST indices (Fig. 1) is likely symptomatic of a characteristic extratropical response to the progressive twentieth Century warming of the Indian Ocean. Such forcing, however, was unable to explain the trend in North Pacific/North American 500 hPa heights evident in full GOGA simulations. We speculate, therefore, that the North Pacific climate trends have been more intimately linked with statistical changes in ENSO fluctuations, rather than the linear trend in SSTs.

The time scale of North Atlantic climate change since 1950 thus appears to have been principally determined by the time scale of Indian Ocean warming. The dynamical processes responsible for the teleconnection

Fig. 12 Time series (1950–99) of January–March simulated Indian Ocean (15°S–15°N, 40°E–110°E) SST (°C) from greenhouse-forced, historical simulations with the NCAR (*top*), ECHAM (*middle*) and HadCM (*bottom*) coupled models (see text for details)



from the tropical Indian Ocean occur on a much shorter time scale, however. To elucidate the nature of this teleconnection, transient AGCM experiments were performed involving a sudden “switch-on” of a +1 °C Indian Ocean SST anomaly. The extratropical response as a whole was found to saturate in about 40 days. The temporal sequence of adjustment began with a subtropical anticyclone over Southeast Asia during the first week, followed by a negative-polarity PNA-response in the second week. Each of these was reconcilable with the atmospheric response to tropical forcing predicted by linear theory. An appreciable North Atlantic response did not emerge until the third week, and it was judged to be inconsistent with simple Rossby wave dispersion. Indirect evidence, based on our analysis of the transient adjustment of the zonal mean zonal wind, suggested that the North Atlantic response was primarily eddy driven. We speculate that the path toward equilibration of the North Atlantic response to Indian Ocean forcing is through the adjustment of the local storm track, though precisely how this occurs is a subject for future research.

5.2 Discussion

To what extent can the above evidence for the importance of Indian Ocean forcing of observed twentieth Century North Atlantic climate change be interpreted as evidence for a regional manifestation of anthropogenic change? Are the structure and statistics of such observed SST changes consistent with a human-induced response of the oceans? Further insight is critical for assessing whether the regional North Atlantic change patterns of the last half-century will persist and perhaps intensify.

The various AGCM experiments we have studied in P1 and here all used climatological values of anthropogenic trace gases and aerosols, so that their capacity to qualitatively explain boreal winter NH climate trends of the last half of the twentieth Century indicates the *direct atmospheric effect* of those greenhouse gases is not a necessary condition. However, the history of prescribed SSTs is likely to bear a footprint of the climate response to changes in the atmospheric chemical composition. Thus, the existence of an *indirect greenhouse effect*

IPCC(A2) Linear Trends SST (JFM) 1975-2024

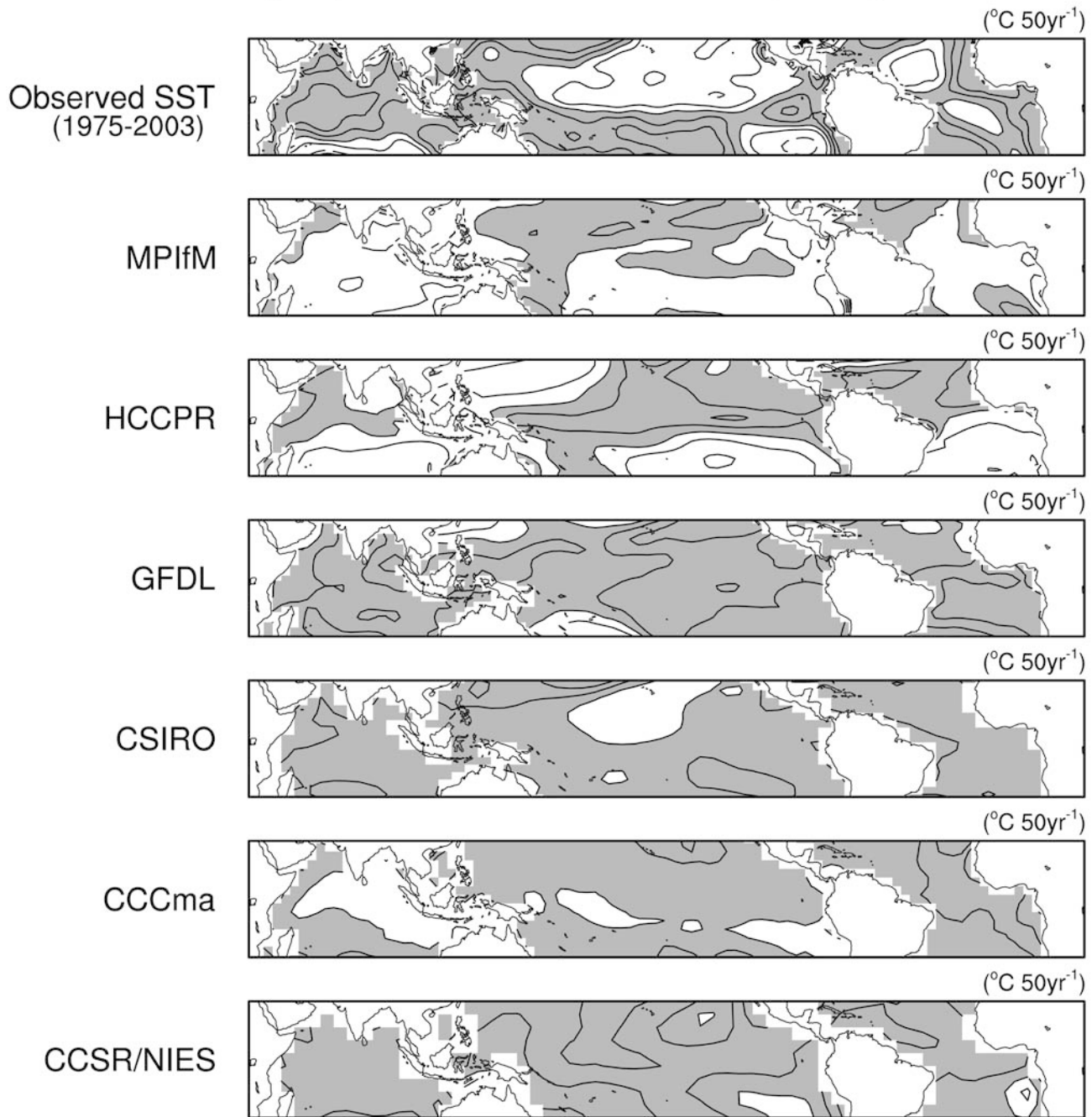


Fig. 13 Linear trends (January–March) of observed (1975–2003) and simulated (1975–2024) tropical SST from six coupled models forced under the A2 emission scenario of the IPCC TAR (2001). The contour increment is $0.3\text{ }^{\circ}\text{C}$ per 50 year, values exceeding

$+0.6\text{ }^{\circ}\text{C}$ per 50 year are *shaded*, negative trends are *dashed*, and the zero contour has been omitted. The model acronyms are those used by IPCC. Details for each model are at: http://ipcc-ddc.cru.uea.ac.uk/dkrz/dkrz_index.html

through dynamical responses to changes in the mean state and statistical properties of the tropical oceans cannot be discounted. Although interdecadal fluctuations are evident, for instance, in long instrumental records of Indian Ocean surface temperatures (Deser et al. 2004), that the recent warming there contains a signature of anomalous greenhouse gas forcing is suggested

through analyses of “historical” integrations with coupled ocean-atmosphere climate models. We examined one such integration in P1, in which the NCAR Climate System Model (CSM; Boville and Gent 1998) was forced with estimates of observed time-dependent changes in sulfate aerosol and greenhouse gas concentrations. In that run, the linear trend of the simulated JFM Indian

Ocean SST time series since 1950 was statistically equivalent to the observed rate of warming over the same period (see Fig. 13 of P1). Moreover, this conspicuous agreement does not appear to arise as a result of a coincidental natural variation in the CSM. Analysis of a long, control integration with this model reveals that the largest increase in tropical Indian Ocean SSTs over any 50 year period of a 1,000 year record is 0.24 °C, which is less than half of the magnitude of the simulated 1950–1999 trend.

Similar behavior is evident in historical simulations with other coupled climate models as well. Figure 12 shows the Indian Ocean SST anomaly time series from the aforementioned CSM integration, together with greenhouse gas forced twentieth Century simulations with the Hadley Centre coupled GCM (HadCM3; Gordon et al. 2000) and the coupled version of the European Centre-Hamburg model (ECHAM; Roeckner et al. 1996). The ability of the greenhouse-forced coupled models to replicate the observed Indian Ocean SST warming over the last half of the twentieth Century is striking. The CSM, ECHAM and HadCM3 simulated trends are 0.55 ± 0.15 °C, 0.67 ± 0.11 °C and 0.69 ± 0.27 °C per 50 years, respectively, compared to the observed trend of 0.60 ± 0.10 °C.

Our theory for an anthropogenic, dynamical oceanic forcing of North Atlantic climate change by Indian Ocean SST anomalies might clarify why neither unforced AGCMs nor unforced coupled models are able to produce winter NAO index trends of the magnitude observed since 1950 (Gillett et al. 2003). But if this tropical warming is the primary prerequisite, and if such regional warming is simulated in most greenhouse gas forced experiments, why then is there a lack of consistency in the North Atlantic response among such coupled model simulations (Cubasch et al. 2001)?

One reason could of course be the small ensemble size of coupled model projections of future climate change, so that internal noise overwhelms the signal. But it is also reasonable to suppose that the spatial pattern of tropical SST change is important, and not just the average SST change over the Indian Ocean alone. Shown in Fig. 13 are the JFM trends in tropical SSTs over 1975–2024 from six coupled models forced under the A2 emission scenario of IPCC (2001). Also shown for comparison is the observed SST trend over the first half (1975–2003) of this period. Local differences are notable, including over the Indian Ocean region. There are also some indications for divergence from nature's trajectory, especially over the east Pacific where the simulated El Niño-like pattern of mean warming is not yet seen. Given the evidence for a tropical SST control of twentieth Century regional climate change, it is important to determine the uncertainty in future regional climate change that may originate from the divergence in projections of future ocean states. Key to such efforts will be advanced understanding of the dynamical responses of the extratropics to various, plausible trajectories of the tropical oceans.

References

- Bader J, Latif M (2003) The impact of decadal-scale Indian Ocean SST anomalies on Sahelian rainfall and the North Atlantic Oscillation. *Geophys Res Lett* 30, DOI 10.1029/2003GL018426
- Boville BA, Gent PR (1998) The NCAR climate system model, version one. *J Clim* 11: 1115–1130
- Cubasch U and Coauthors (2001) Projections of future climate change. In: Houghton JT, Ding Y, Griggs DJ, Noguer M, van der Linden PJ, Xiaosu D (eds) *Climate change 2001, the scientific basis*. Cambridge University Press, Cambridge UK pp 525–582
- Deser C, Phillips AS, Hurrell JW (2004) Pacific interdecadal climate variability: linkages between the tropics and North Pacific in boreal winter since 1900. *J Clim* (in press)
- Ferrara JD, Mechoso CR, Robertson AW (2000) Ensembles of AGCM two-tier predictions and simulations of the circulation anomalies during winter 1997–98. *Mon Weather Rev* 128: 3589–3604
- Gillett NP, Graf HF, Osborn TJ (2003) Climate change and the North Atlantic Oscillation. In: Hurrell JW, Kushnir Y, Ottersen G, Visbeck M (eds) *The North Atlantic Oscillation: climatic significance and environmental impact*. *Geophys Monogr* 134: 193–209
- Gordon C, Cooper C, Senior CA, Banks H, Gregory JM, Johns TC, Mitchell JFB, Wood RA (2000) The simulation of SST, sea ice extents and ocean heat transports in a version of the Hadley Centre coupled model without flux adjustments. *Clim Dyn* 16: 146–168
- Hoerling MP, Kumar A (2003) The perfect ocean for drought. *Science* 299: 691–694
- Hoerling MP, Hurrell JW, Xu T (2001) Tropical origins for recent North Atlantic climate change. *Science* 292: 90–92
- Hurrell JW, Trenberth KE (1999) Global sea surface temperature analyses: multiple problems and their implications for climate analysis, modeling, and reanalysis. *Bull Am Meteorol Soc* 80: 2661–2678
- Hurrell JW, Hoerling MP, Phillips AS, Xu T (2004) Twentieth Century North Atlantic climate change. Part I. Assessing determinism. *Clim Dyn* (in press)
- IPCC (2001) *Climate change 2001, the scientific basis*. Houghton JT, Ding Y, Griggs DJ, Noguer M, van der Linden PJ, Xiaosu D (eds) Cambridge University Press Cambridge UK pp 881
- Kiehl JT, Hack JJ, Bonan GB, Boville BA, Williamson DL, Rasch PJ (1998) The National Center for Atmospheric Research Community Climate Model: CCM3. *J Clim* 11: 1131–1149
- Lee S, Kim H-K (2003) The dynamical relationship between subtropical and eddy driven jets. *J Atmos Sci* 60: 1490–1503
- Lin H, Derome J, Greatbatch RJ, Peterson KA, Lu J (2002) Tropical links of the Arctic Oscillation. *Geophys Res Lett* 29, DOI 10.1029/2002GL015822
- Lu J, Greatbatch RJ, Peterson KA (2004) On the trend in northern hemisphere winter atmospheric circulation during the last half of the 20th Century. *J Clim* 17: (in press)
- Mehta V, Suarez M, Manganello JV, Delworth TD (2000) Oceanic influence on the North Atlantic Oscillation and associated Northern Hemisphere climate variations: 1959–1993. *Geophys Res Lett* 27: 121–124
- Pegion P, Suarez M, Schubert S (2001) An analysis of the causes of differences in circulation patterns during the El Niño winters of 1983 and 1998. 26th Annual Climate Diagnostics and Prediction Workshop, La Jolla, CA. National Oceanic and Atmospheric Administration
- Reynolds RW, Smith TM (1994) Improved global sea surface temperature analyses using optimum interpolation. *J Clim* 7: 929–948
- Robinson W (1992) Predictability of the zonal index in a global model. *Tellus* 44A: 331–338
- Robinson WA (1996) Does eddy feedback sustain variability in the zonal index? *J Atmos Sci* 53: 3556–3569

- Rodwell MJ, Rowell DP, Folland CK (1999) Oceanic forcing of the wintertime North Atlantic Oscillation and European climate. *Nature* 398: 320–323
- Roeckner E, and Coauthors (1996) The atmospheric general circulation model ECHAM4: model description and simulation of present-day climate. Max Planck Institut für Meteorologiem Report 218, Hamburg, Germany, pp 90
- Schubert SD, Suarez MJ, Pegion PJ, Koster RD, Bacmeister JT (2003) Causes of long-term drought in the United States Great Plains. *J Cim* 17: 485–503
- Schneider EK, Bengtsson L, Hu Z.-Z (2003) Forcing of Northern Hemisphere climate trends. *J Atmos Sci* 60: 1504–1521
- Simmons AJ, Wallace JM, Branstator G (1983) Barotropic wave propagation and instability, and atmospheric teleconnection patterns. *J Atmos Sci* 40: 1363–1392
- Smith TM, Reynolds RW, Livezey RE, Stokes DC (1996) Reconstruction of historical sea surface temperatures using empirical orthogonal functions. *J Clim* 9: 1403–1420
- Sutton RT, Hodson DLR (2003) The influence of the ocean on North Atlantic climate variability 1871–1999. *J Clim* 16: 3296–3313
- Sutton RT, Norton WA, Jewson SP (2001) The North Atlantic Oscillation - what role for the ocean? *Atmos Sci Lett* DOI 10.1006/asle.2000.0018
- Thompson DWJ, Wallace JM, Hegerl GC (2000) Annular modes in the extratropical circulation, Part II: trends. *J Clim* 13: 1018–1036
- Thompson DWJ, Lee S, Baldwin MP (2003) Atmospheric processes governing the Northern Hemisphere Annular Mode/ North Atlantic Oscillation. In: Hurrell JW, Kushnir Y, Ottersen G, Visbeck M (eds) *The North Atlantic Oscillation: climatic significance and environmental impact*. *Geophys Monogr* 134: 81–112
- Ting M, Yu L (1998) Steady response to tropical heating in wavy linear and nonlinear baroclinic models. *J Atmos Sci* 55: 3565–3582
- Trenberth KE, Branstator GW, Karoly D, Kumar A, Lau N.-C, Ropelewski C (1998) Progress during TOGA in understanding and modeling global teleconnections associated with tropical sea surface temperatures. *J Geophys Res* 103: 14,291–14,324
- Venzke S, Allen MR, Sutton RT, Rowell DP (1999) The atmospheric response over the North Atlantic to decadal changes in sea surface temperatures. *J Clim* 12: 2562–2584